RSC Applied Interfaces

ROYAL SOCIETY OF CHEMISTRY

PAPER

View Article Online
View Journal | View Issue

Cite this: *RSC Appl. Interfaces*, 2026, **3**, 485

Synergy or interference? The effect of electrolyte additives and formation protocols combined in sodium-ion batteries

Katja Lahtinen, * Paul Latis, Lucas Bruylands and Guiomar Hernández *

Sodium bis(oxalato)borate in triethyl phosphate (NaBOB–TEP) is a promising fluorine-free non-flammable electrolyte for sodium-ion batteries, though it suffers from irreversible capacity losses during the first cycle due to the reduction of NaBOB. Here, the effects of the passivating electrolyte additives and different formation protocols on the electrolyte performance are investigated. The normal formation protocol is based on slow C-rate while the skip protocol has a high C-rate step until 3 V to bypass the NaBOB decomposition. The skip protocol is proved to be more effective in improving the initial coulombic efficiency of 0.35 M NaBOB–TEP than the additives but in the long-term cycling the effect is evened. The cyclic voltammetry results show that during normal formation the additives 1,3,2-dioxathiolane 2,2,-dioxide (DTD) and prop-1-ene-1,3-sultone (PES) are reduced before NaBOB which stabilizes the solid electrolyte interphase (SEI) and the cell cycling. On the other side, the skip protocol bypasses the positive SEI formation capability of PES and DTD, preventing the traditional SEI formation. Meanwhile, the less reactive 1,4-butane sultone (BS) additive that is not able no prevent NaBOB decomposition on its own, benefits from the changes in the formation step similarly to the baseline electrolyte, and this combined with a small amount of sulphur in the SEI from the BS decomposition, results in the best cycling performance when the skip protocol is used. The results indicate that if additives and skip protocol are used together, the investigation for the best-performing additive should be done using the intended cycling protocol, because the protocol affects the additive performance as well.

Received 23rd December 2025,
Accepted 4th February 2026

DOI: 10.1039/d5lf00401b

rsc.li/RSCApplInter

Introduction

Sodium-ion batteries (SIB) are an alternative to lithium-ion batteries (LIB) thanks to the high abundance of sodium and lower dependence on other critical elements such as cobalt, thus making them cheaper and more environmentally friendly. However, besides the active materials, there are other components that compromise safety and sustainability, such as the electrolyte.

The state-of-the-art electrolytes used in SIB are inherited from LIB technology and typically consist of a fluorine containing salt, such as $NaPF_6$ or sodium bis(trifluoromethanesulfonyl)imide (NaTFSI), dissolved in a mixture of carbonate-base solvents, often ethylene carbonate (EC) and diethyl carbonate (DEC). However, carbonates are flammable and often one of the biggest safety hazards in the battery. In addition, fluorine is problematic from the sustainability perspective, as the decomposition of the salts often lead to the formation of toxic and corrosive chemicals, such as phosphorus pentafluoride, phosphoryl fluoride and fluorides, including hydrofluoric acid.[1] In addition, recycling of fluorine species is often difficult as they damage the reactors or remain as impurities.[2] The use of fluorine-containing salts is often justified with their good ionic conductivities, good ionic dissociation and their ability to passivate the aluminium current collector. However, it has recently been shown that alternatives with similar properties exist,[3] and that the use of fluorine-based anions is not as well-justified as it was before.

One of the most studied non-fluorinated electrolytes is based on sodium bis(oxalato)borate (NaBOB). It is both thermally stable, relatively cheap and low in toxicity, making it an attractive non-fluorinated alternative. The major challenge of NaBOB is its poor solubility in most organic solvents, which in turn limits the ionic conductivity of the electrolytes that use it. In terms of alternative non-flammable solvents, TEP is gaining attention due to its low cost and environmental friendliness. However, this solvent co-intercalates into graphite,[4] which partially restricts its use for lithium-ion batteries. However, as sodium-ion batteries use hard carbon (HC) as the negative electrode

Department of Chemistry – Ångström Laboratory, Uppsala University, Box 538, SE-751 21 Uppsala, Sweden. E-mail: katja.lahtinen@kemi.uu.se, guiomar.hernandez@kemi.uu.se

and the amount of graphitic carbon is smaller, the issue is not as large.

In recent years, the combination of NaBOB with TEP as a fluorine-free non-flammable electrolyte has been investigated. Colbin *et al.*[5] reported the solubility of NaBOB up to 0.38 M in TEP with the ionic conductivity of 5 mS cm^{-1}, a competitive value within Na-ion electrolytes. This study identified that the formation of a proper solid electrolyte interphase (SEI) layer is the main challenge of this electrolyte, which then led to efforts to understand and improve it. First, Welch *et al.*[6] investigated the effect of additives on improving the SEI formation and observed improved coulombic efficiency (CE) during the initial charge–discharge cycles. Then Buckel *et al.*[7] observed that modifying the formation protocol and starting with a high C-rate step (10C until 3.0 V and constant voltage for 1 h) to avoid the NaBOB decomposition (a so-called skip protocol) and increasing the temperature during formation both improve the CE as well.

In this study we investigate how the formation protocol affects the SEI-forming properties of the additives and how the combination could have both positive and negative effects. The cell chemistry is Prussian white (PW)–HC and 0.35 M NaBOB–TEP as electrolyte baseline. Passivation layer forming additives with different structures are investigated, some of them based on promising previous results.[6] Sulphur-based additives are 1,4-butane sultone (BS), 1,3,2-dioxathiolane 2,2-dioxide (DTD) and prop-1-ene-1,3-sultone (PES). Out of these, DTD and PES have previously been shown to improve the NaBOB–TEP performance,[6] though the mechanism is not well understood. Based on the results in other electrolyte systems,[8] the opening of the sulphur-containing ring is speculated to be the cause for a more stable SEI and better performance. Because of this, a third ring-structured sulphur-containing additive, BS, was selected for the matrix. BS differs from the other two sulphur-containing additives by having a 6-membered ring instead of a 5-membered, and it could therefore have a different reaction mechanism. The goal of comparing BS to the other two was to investigate the effect of the ring size and how it would affect the SEI formation with the different protocols. In order to investigate the effect of the sulphur, we also selected two ring-structured additives without sulphur. Vinyl ethylene carbonate (VEC) was selected because of its resemblance to vinylene carbonate (VC), a well-known electrolyte additive. VC was previously shown to affect the NaBOB–TEP system negatively,[6] and was therefore excluded from this study. Trimethoxy-boroxine (TMB) was chosen due to its positive electrode stabilizing properties[9] and its boron-containing structure. To help understand the cause of the performance differences of these additive systems, cyclic voltammetry (CV), scanning electron microscopy (SEM) and X-ray photoelectron spectroscopy (XPS) measurements are performed on the hard carbon electrodes. We show that modifying the formation protocol is beneficial for the baseline electrolyte NaBOB–TEP but it competes with the positive effects of the well-known SEI forming additives, such as PES. On the other hand, less reactive additives, such as BS, not able to passivate the anode's surface during the normal formation protocol, show improvement with the new formation protocol. Furthermore, we observe a different sodiation mechanism with the NaBOB–TEP system which correlates with the competitive effect observed between SEI forming additives and formation protocols.

Materials and methods

Sodium bis(oxalato)borate was synthesized in water using oxalic acid (Sigma-Aldrich, ReagentPlus® ≥99%), boric acid (Sigma-Aldrich, ACS reagent ≥99.5%) and sodium hydroxide (Sigma-Aldrich, reagent grade ≥98%) according to the procedure reported by Zavalij *et al.*[10] The obtained product was recrystallized in isopropanol (VWR) and trimethyl phosphate (Sigma-Aldrich, for synthesis) in a volumetric ratio of 2 : 1 and the collected crystals were dried in vacuum at 120 °C for 20 hours. The synthesized NaBOB was characterized with X-ray diffraction (XRD, Siemens D5000, Bragg–Brentano, Cu $K\alpha_1$, 45 kV, 40 mA), Fourier-transmission infrared spectroscopy (FTIR, Bruker, Vertex 70v), thermogravimetric analysis (TGA, TA Instruments, TG5500) and scanning electron microscopy (Zeiss, LEO 1530, 3 kV, in-lens detector).

The electrolyte solutions were prepared by dissolving the synthesised NaBOB in triethyl phosphate (Sigma-Aldrich, ReagentPlus® ≥99.8%) in Ar-filled glovebox (O_2 < 1 ppm, H_2O < 0.2 ppm) overnight at room temperature and then at 50 °C for 2 h. The additives were purchased from commercial sources, PES and VEC from Tokyo Chemical Industry and BS, DTD and TMB from Sigma-Aldrich. The amount of additive added to the electrolyte was kept constant, always at 2 wt%. The density and viscosity of the solutions were investigated using a density meter (Anton Paar, DMA4100M) and the water content of the solutions was checked with Karl-Fischer titration (Metrohm, 851 Titrando). The ionic conductivities of the solutions were tested using a probe from Mettler Toledo (SevenCompact Duo). The solvation structure of the electrolytes was investigated with FTIR (specifics above) and nuclear magnetic resonance (NMR) spectroscopy measurements with Jeol Resonance ECZ400S and Agilent 400-MR instruments. Deuterated dimethyl sulfoxide (DMSO-d_6, VWR, NMR spectronorm® 99.80%) was used as a solvent for the NMR impurity studies, and a separated tube of 1 m NaCl (≥ 99.5%, Fisher Chemical) dissolved in deuterium oxide (99.9%, Sigma-Aldrich) as a reference for studying the solvation in the samples.

Pouch cells were assembled to test the electrochemical performance of the electrolytes. The positive electrode of the full cell pouches consisted of 85 wt% Prussian white (Fennac, Altris AB), 10 wt% active carbon (Timcal Ensaco 250 P) and 5 wt% carboxymethyl cellulose (CMC, Daicel FineChem, 2200). The negative electrode consisted of 95 wt% hard carbon (Kuraray, Kuranode Type 2 (5 μm)) and 5 wt% CMC. The active material mass-loading on the positive electrode was

4.8–6.4 mg cm^{-2} and 2.6–3.5 mg cm^{-2} on the negative electrode while the electrode diameters were 13 mm and 14 mm, respectively. The capacity ratio of the negative/positive electrodes was 1.1. Carbon-coated aluminium (Shohoku Laminate) was used as current collector in both electrodes, Dreamweaver Gold (23 μm thickness, 2 cm × 2 cm area) as the separator and the amount of electrolyte was 100 μl for two-electrode cells and 150 μl for three-electrode cells.

Partly desodiated Prussian white electrodes of approximately 3.3 V *vs.* Na^+/Na (determined independently for each reference) and with a shape of a semicircle with a diameter of 14 mm were used as the reference electrodes in the three-electrode cells. The reference electrodes were prepared by assembling a full cell, formatting them with the normal formation protocol (detailed below) and then charging the cell to the desired voltage. The electrolyte in these cells had the same salt–solvent combination as the upcoming three-electrode measurements, but without the additives. After the cell was stabilized, it was disassembled and the partly desodiated PW electrode extracted and cut to half to use the same reference in two cells. The electrode was not washed but assembled to the new cell as it was.

The galvanostatic rate capability and long-term cycling tests were done with a Neware cycler in the voltage range of 1.3–3.8 V using two-electrode cells. For each electrolyte composition and test, at least three parallel samples were measured, and the most average sample selected for the figures. The C-rate for the normal formation was 0.1C with constant-current constant-voltage (CCCV) charge and discharge with the cut-off current at 0.03C. For the skip protocol formation, the cells were first charged at 7C until 3.0 V (CCCV, cut-off 0.1C) after which the C-rate was to 0.1C (CCCV to 3.8 V, cut-off 0.03C). The discharge C-rate was 0.1C (CCCV, cut-off 0.03C). After this, both the normal and skip protocol cells were cycled with constant current (CC) of 0.1C for five more cycles before the actual measurement was started. The long-term cycling program consisted of cycling the cells with CC of 0.2C for 200 cycles. In the rate capability program the cells were cycled five times with CC C-rates of 0.2C, 0.5C, 1.0C, 2.0C, 4.0C, 5.0C and finally once more with 0.2C. The polarisation values were determined by calculating the difference in voltage between the charge and discharge curves at 40 mAh g^{-1} from the upper cut-off voltage, similarly to the study by Welch *et al.*[6]

The cyclic voltammetry was performed with a Biologic (MPG2) potentiostat using three-electrode cells to investigate the electrochemical stability window and SEI formation. The scan rate was 0.05 mV s^{-1}. Hard carbon was used as the working electrode to investigate realistic SEI formation, PW as the counter electrode and desodiated PW as the reference electrode.

Hard carbon pristine, soaked and formatted, fully sodiated electrodes were analysed using SEM (information above) and X-ray photoelectron spectroscopy (Kratos, Super Plus) with photon excitation energy of 1487 eV (Al Kα). The soaked samples were prepared by assembling pouch cells normally and disassembling them after 24 hours to collect the electrodes. The formatted samples were prepared by cycling them with the skip protocol (one cycle) described above. The soaked and cycled cells were disassembled in the glovebox, and the electrodes, including the pristine ones, were then dried at room temperature under vacuum for 3 hours (without washing). The SEM samples were exposed to air for approximately 30 minutes during the sample transport to the instrument. The XPS samples on the other hand were transferred to the instrument in a vacuum-sealed sample holder, and thus they were not exposed to air. The binding energies in the recorded XPS spectra were calibrated with the sp^2 C=C peak of hard carbon placed at 284.5 eV for pristine and soaked samples, and the sp^3 C–C peak at 284.8 eV for the formatted samples. The intensity of the peaks was not normalized.

Results

NaBOB is a non-fluorinated salt that until recently has not been available commercially. For this work it was synthesized as described in the experimental section and the crystals were analysed using XRD, FTIR, ^{13}C NMR, TGA and SEM. The results have been collected in Fig. S1–S5 and they show that the synthesized NaBOB has good quality and behaves as previously reported in the literature. Once the structure and purity were confirmed, 0.35 M NaBOB was dissolved in TEP as the baseline electrolyte, and the water content investigated with Karl-Fischer titration was determined to be 20 ppm.

Five additives with different chemical structures and functionalities were investigated as additives with 2 wt% for the NaBOB–TEP system. These were 1,4-butane sultone (BS), 1,3,2-dioxathiolane 2,2-dioxide (DTD) and 1,3-propene sultone (PES) as cyclic sulfur containing additives, vinyl ethylene carbonate (VEC) as an alternative to the well-known vinylene carbonate (VC) that does not work well in NaBOB–TEP system,[6] and trimethoxy boroxine (TMB) that has been reported to improve positive electrode stability in LIBs.[9] The chemical structures of the electrolyte components including NaBOB, TEP and all the additives are presented in Fig. 1.

After the electrolytes were prepared, their physical properties were explored. The ionic conductivities of the 0.35 M NaBOB–TEP electrolytes containing 2 wt% of different additives were measured at 21.5 °C and the results are presented in Table 1. The ionic conductivity of our baseline electrolyte without additives is 4.1 mS cm^{-1}. As a reference, the ionic conductivity of $NaPF_6$ in carbonates is between 7–8 mS cm^{-1}.[11] Despite the lower value, the baseline electrolyte has shown good performance in previous studies, suggesting that it is still within a reasonable range for battery applications. The additives seem to improve the ionic conductivity slightly but not notably, and the differences are almost within the margin of error. The biggest improvement is obtained using trimethoxy boroxine (TMB) as the additive, resulting in the ionic conductivity of 4.5 mS cm^{-1}. The cause

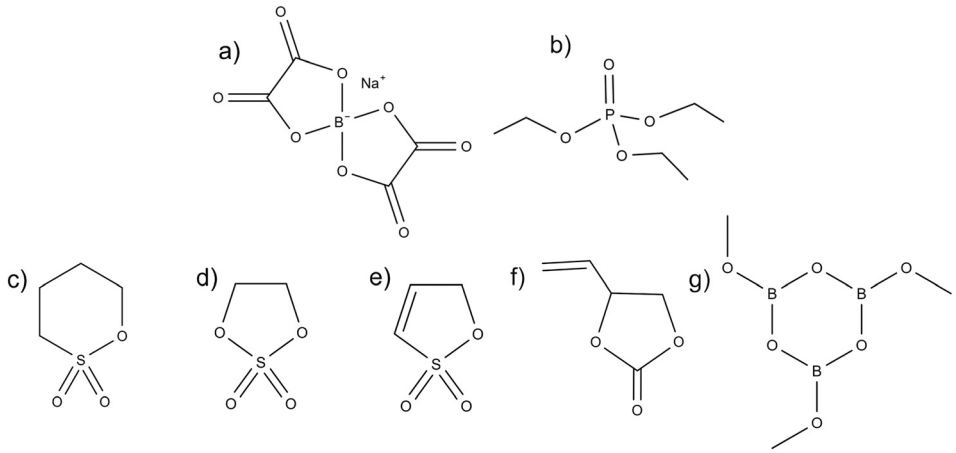

Fig. 1 The chemical structures of a) sodium bis(oxalato)borate (NaBOB), b) triethyl phosphate (TEP), c) 1,4-butane sultone (BS), d) 1,3,2-dioxathiolane 2,2-dioxide (DTD), e) 1,3-propene sultone (PES), f) vinyl ethylene carbonate (VEC), and g) trimethoxy boroxine (TMB).

for the small changes could not be verified within the scope of this work.

To further understand the physical properties of the electrolyte solutions, their viscosity and density were measured and the results are reported in Fig. 2a and b. Generally, it is observed that 2 wt% of the additive does not affect the physicochemical properties of the electrolyte considerably. At room temperature, all samples show the kinematic viscosity of 2.2 $mm^2\ s^{-1}$ and the density between 1.11–1.12 $g\ cm^{-3}$. As expected, both the viscosities and the densities of the electrolytes increase with decreasing temperature and decrease with increasing temperature.

In addition, the electrolytes were also analysed with FTIR and NMR to investigate how the additives affect the solvation structure of the NaBOB–TEP electrolyte. The enlargement of the P═O stretch at 1265 cm^{-1} in the FTIR spectra (Fig. 2c, whole spectra in Fig. S6) shows the formation of a new peak at 1295 cm^{-1} when NaBOB is dissolved in TEP. This is attributed to the coordination of Na^+ by the double-bonded oxygen in TEP during the NaBOB salt solvation. However, no additional changes are observed in the P═O stretch caused by the additives. The ^{31}P NMR studies (Fig. 2d) support the results from the FTIR. Upon the solvation of NaBOB, the TEP phosphorus peak is shifted 0.37 ppm upfield, resulting from a greater d-orbital occupancy in the P–O bonds when Na^+ is coordinated to TEP.[12] Shifts caused by NaBOB solvation are also observed in the ^{23}Na and ^{17}O NMR (Fig. S7), supporting the results seen in ^{31}P NMR. Yet, when the additive-containing samples are compared to the NaBOB–TEP baseline, no changes are observed, which could be due to the relatively low concentration of the additives.

Table 1 Ionic conductivities of the 0.35 M NaBOB–TEP electrolytes containing 2 wt% of different additives measured at 21.5 °C. The measurement margin of error is 0.2 mS cm^{-1}

	Baseline	BS	DTD	PES	VEC	TMB
Conductivity (mS cm^{-1})	4.1	4.2	4.3	4.3	4.4	4.5

In the previous studies with NaBOB, it has been shown to reduce on the negative electrode at approximately 1.2 V *vs.* Na^+/Na. In the full cell with Prussian white and hard carbon electrodes, this results in a plateau at 1.7 V.[5] This decomposition is assumed to be part of the reason why the coulombic efficiency of the NaBOB–TEP system during the first cycle is relatively low, for example 76% in the work by Welch *et al.*[6] In the recent work by Buckel *et al.*,[7] using a higher current during the first step of the formation charge was observed to prevent part of this NaBOB decomposition and the coulombic efficiency of the first cycle improved to 85%. Similarly, Welch *et al.*[6] were able to improve the CE with several SEI forming additives. While changing the formation protocol and using additives have been shown to be effective in improving the baseline NaBOB–TEP independently, here we investigate how the formation protocols affect the additive's SEI forming properties, and how that affects the cycling performance. Therefore, two different formation protocols were performed for PW–HC pouch cells. In the first protocol called "normal" the cell was cycled at a C-rate of 0.1C with constant current constant voltage (CCCV) to the respective charge and discharge voltage cut-offs and held at that voltage until the current dropped to 0.03C. In the second protocol inspired by Buckel *et al.*[7] and called "skip", the cells were first charged to 3.0 V with the C-rate of 7.0C and kept there until the current dropped to 0.1C. After this the formation continued at 0.1C with the same CCCV-parameters as in the first protocol. The skip protocol differs from Buckel's protocol followingly: in their case the high C-rate was set to 10C and the constant voltage hold at 3.0 V was restricted to 1 h, regardless of the current reached.

The behaviour of the NaBOB–TEP-additive systems during these two formation protocols is compared in Fig. 3. The charge–discharge voltage curves with the normal protocol are compared in Fig. 3a and b and the ones with the skip protocol in Fig. 3c. Individual plots of each sample can be found in Fig. S8 and S9. All the charge curves with the

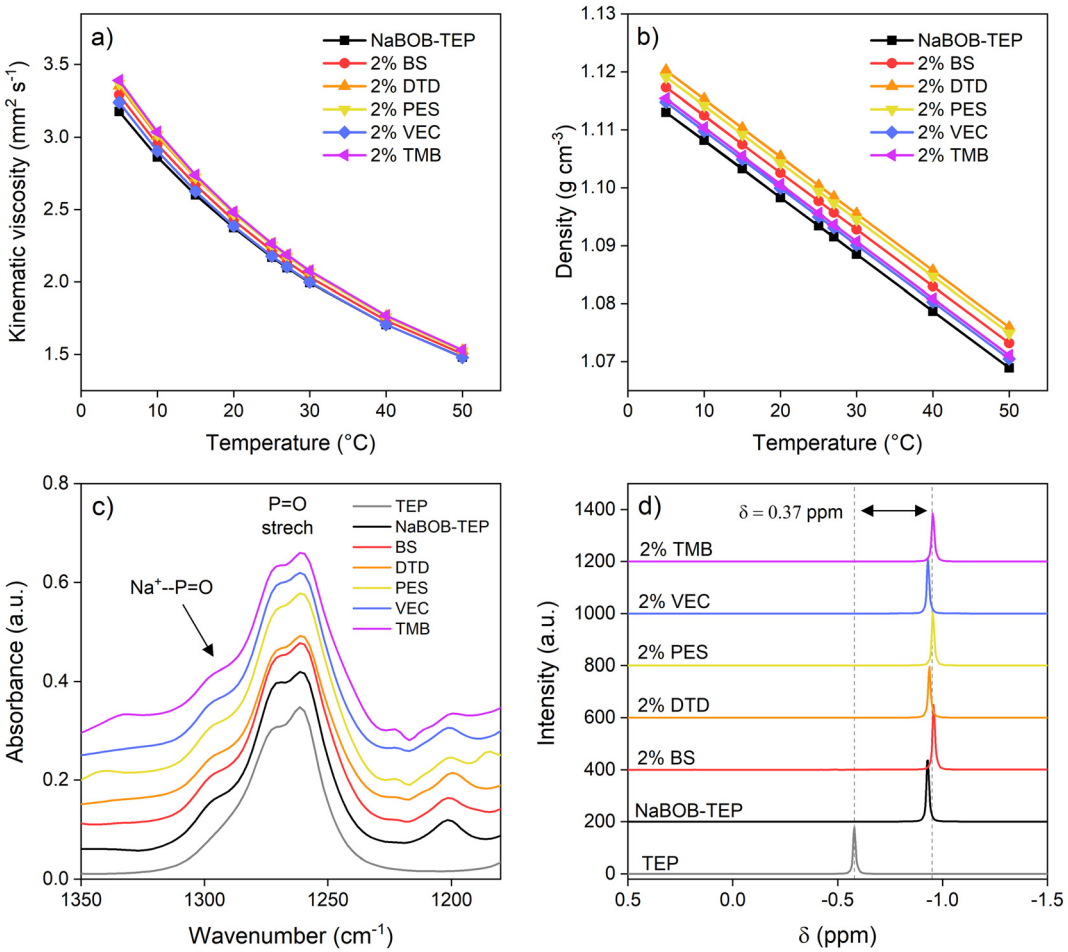

Fig. 2 Physicochemical properties of the 0.35 M NaBOB–TEP electrolytes containing 2 wt% of different additives. Dependency of a) kinetic viscosity and b) density on temperature for electrolytes. c) FTIR spectra of the TEP P═O stretch, and d) ^{31}P NMR spectra of the electrolytes.

normal protocol contain the typical sloped incline between 2.5 V and 3.0 V caused by the summarized effect of the HC sodiation[13,14] and PW desodiation,[15] and a plateau around 3.3 V caused by the second desodiation phase transformation of PW. In addition, an extra plateau is observed around 1.7 V, which, as previously mentioned, is attributed to the decomposition of the NaBOB salt. In the skip protocol charge curves (Fig. 3c) the 1.7 V plateau and the 2.5–3.0 V incline are bypassed and instead the voltage is forced to stay at 3.0 V until the current reaches 0.1C. After this, the second PW plateau is more or less similar to the normal protocol. It can be observed that during the normal formation protocol, DTD and PES, the two sulphur-containing additives with the five-member ring structure, diminish the plateau at 1.7 V, indicating a decrease in the NaBOB decomposition. This is emphasized in the dQ/dV plots in Fig. 3d with a decrease in the peak at around 1.7 V compared to the baseline electrolyte. The other additives do not affect the charge curves, suggesting that they do not prevent the NaBOB decomposition. This is intriguing, because for example BS is a sulphur-containing cyclic compound similarly to DTD and PES, and we were expecting similar behaviour. This is not the case, however, and we will discuss the matter more in connection to the CV results. It should be noted, however, that the polarisation in the BS electrolyte is slightly smaller compared to other samples, which indicates that resistance in the BS cells is lower. TMB is not observed to affect the NaBOB decomposition but it does affect the charge by increasing the cell voltage during the first incline making it resemble more PW first sodiation phase transition.[15] This suggests that TMB has an effect on the hard carbon sodiation process, decreasing the potential of the first part of the sodiation. This is confirmed and discussed later with the CV results. When the skip protocol is used, the effect of the additives cannot be observed in the beginning of the charge curves, as they are covered by the constant voltage step of the protocol at 3 V. It is observed, however, that the TMB containing system reaches the end of the 3.0 V—hold earlier than other systems, with the voltage curve afterwards quite similar to its normal formation protocol. It is also worth mentioning that despite the differences in the charge curves, the discharge curves for all the additives and with both protocols look quite similar in shape, as well as all

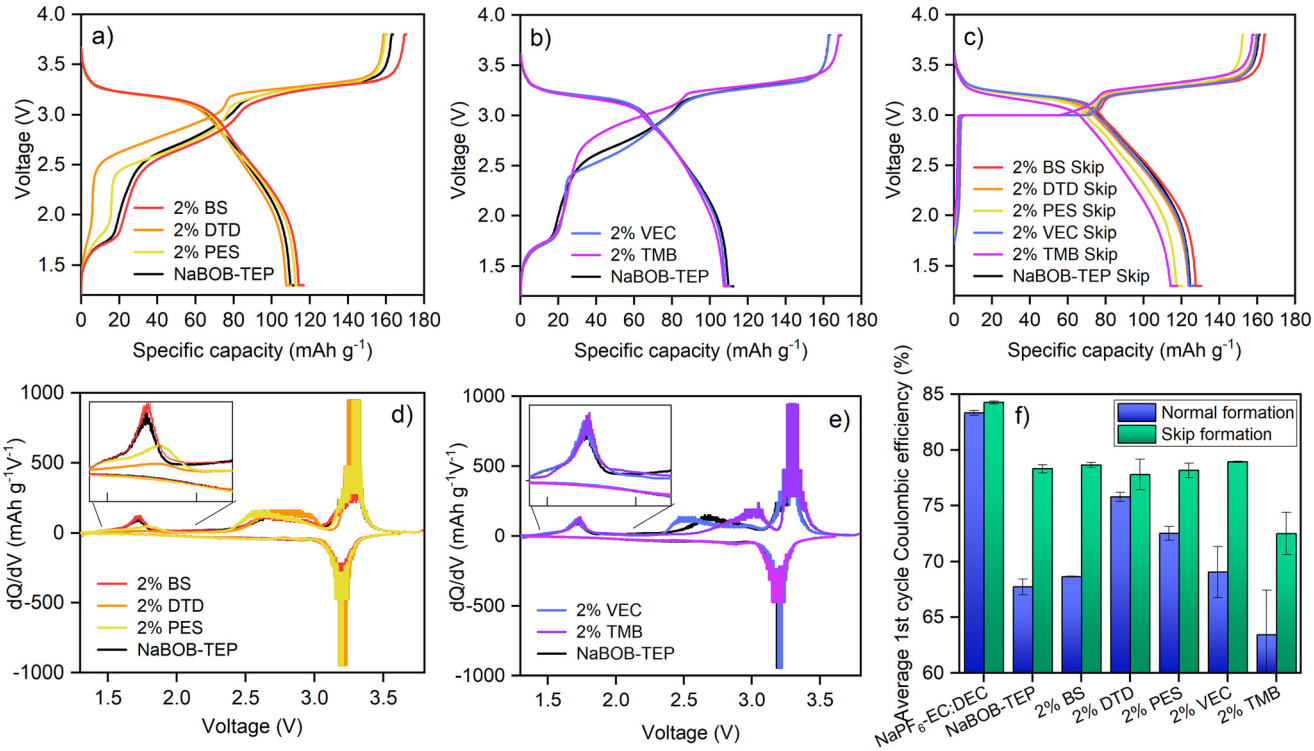

Fig. 3 Comparison of Prussian white–hard carbon cell formation using 0.35 M NaBOB–TEP electrolyte with additives and two different formation protocols. Charge–discharge voltage curves for the normal protocol with electrolytes containing a) 2 wt% of BS, PES and DTD, and b) 2 wt% of VEC and TMB. c) The charge–discharge voltage curves for the skip protocol with all electrolyte systems. d) The d*Q*/d*V* plots corresponding to the charge–discharge voltage curves for d) 2 wt% of BS, PES and DTD, and e) 2 wt% of VEC and TMB. Insets show the magnified NaBOB decomposition peaks for each electrolyte system. f) Average initial coulombic efficiencies from the normal and the skip protocols with all electrolytes compared to 1 M $NaPF_6$ in EC:DEC.

the charge–discharge curves from the second cycle onwards (Fig. S10 and S11).

The charge–discharge curves also show that similarly to the work by Buckel *et al.*,[7] the skip protocol improves the first cycle discharge capacity of the cells. Generally, each electrolyte system is improved by approximately 10 mAh g^{-1} with the skip protocol expect for the PES system, which has a similar capacity in both normal and skip protocol. The effect of the additives and the formation protocol on the NaBOB–TEP system is also reflected in the coulombic efficiencies of the first cycle, presented in Fig. 3f. When the normal formation protocol is used, the additives have a large effect on the CEs, with DTD and PES improving it from 68% of the baseline to 76% and 73%, respectively, VEC and BS not having a large impact in any direction and TMB decreasing it. This result agrees with the observations in the charge curve, suggesting that decreasing the NaBOB decomposition is beneficial to the system. In comparison, the CE of $NaPF_6$–EC:DEC with normal formation is 84%. The skip protocol on the other hand increases the CE for all the systems. However, the effect of the additives is barely noticeable, and all NaBOB–TEP systems, including the baseline and except for the TMB electrolyte, have very similar CE of approximately 78% regardless of the additive used. As the baseline system is improved more by the skip protocol than with the additives, and also not further improved by the additives, it can be concluded that for gaining capacity during the first cycle for the NaBOB–TEP system, modifications on the cycling protocol provide better results than using additives.

To investigate the effect of the formation protocols with the additives on the cycling, galvanostatic cycling tests were performed with both protocols and all electrolytes, and the results are presented in Fig. 4. As the formation cycle results in Fig. 3 showed, the initial discharge capacity of the cells formatted with the skip protocol is higher. After the formation, 5 additional cycles were done with CC 0.1C, after which the C-rate was increased to 0.2C for the cycling. The capacity drops in all the NaBOB–TEP systems during these five cycles regardless of the additive or the formation protocol. However, it is observed that the drop after the skip formation protocol is larger, suggesting perhaps that the electrolyte is decomposed further after the skip protocol. This indicates that the formation of the NaBOB–TEP systems is not finished only after one cycle but that several cycles are required to stabilize it.

The cycling stability of the 0.35 M NaBOB–TEP without additives is shown to be improved by the skip protocol during approximately the 70 first cycles with a more rapid decay afterwards. Regardless of the formation protocol used, the cells with the baseline electrolyte feature similar capacity retention of 34.2% and 35.8% after 200 cycles for the normal and the skip protocol, respectively. This performance is worse

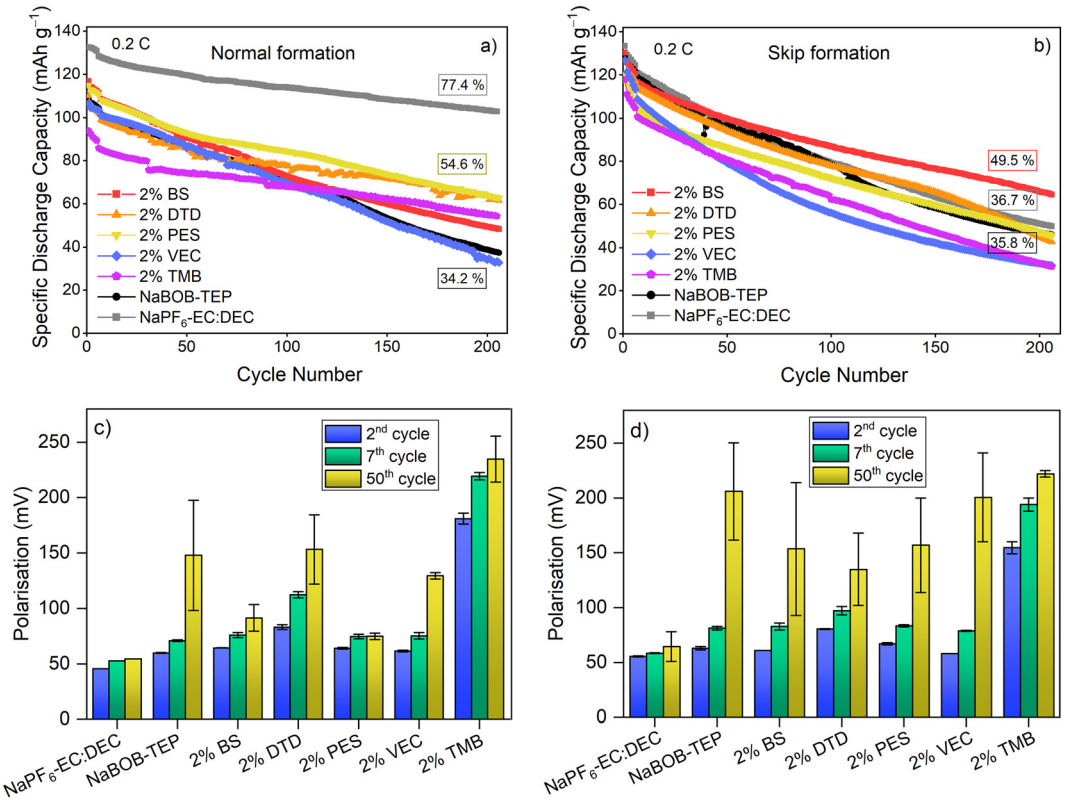

Fig. 4 Galvanostatic cycling of the NaBOB–TEP electrolyte systems with additives in PW–HC pouch cells at 0.2C. a) Cycle life after the normal formation protocol, and b) cycle life after the skip formation protocol. Polarisation of the cells formatted with c) the normal formation and d) the skip formation protocol at 2nd (0.1C) 7th (1st 0.2C cycle) and 50th cycle (0.2C). The values were calculated as the voltage difference between the charge and the discharge curves at 40 mAh g^{-1} from the upper cut-off voltage. The error bars mark the standard error of the replicated samples.

than in the work by Buckel *et al.*,[7] but one has to consider that their measurements were done using commercially optimized electrodes and at elevated temperatures. Nevertheless, this work focuses on the effect of the additives with the formation protocols and the corresponding decomposition reactions, rather than in the long-term cycling performance. With the normal formation protocol, 2 wt% PES system shows the most stable performance after 200 cycles, giving the capacity retention of 54.6%. The system with 2 wt% DTD is also able to reach similar retention at this point; however, its initial capacities are lower and the capacity slightly fluctuates during cycling. The improved performance of PES and DTD is attributed to their ability to reduce and diminish the NaBOB decomposition as observed already in Fig. 3a and will be further shown with the CV measurements. This is also in agreement with previous publications.[16,17] In addition to PES and DTD, BS and TMB also improve the capacity retention after 200 cycles compared to the baseline, though less than the previous two, while VEC performs very similarly to the baseline electrolyte. Interestingly, although the TMB system shows a considerably lower discharge capacity than the other systems due to its poor initial CE, its capacity retention and stability afterwards are relatively good, 57.8%. This suggests that while the electrode passivation consists of more irreversible reactions, it results in a stable system.

With the skip formation protocol the cycling performance of the additive systems changes. PES and DTD were able to improve the capacity retention with the normal protocol, but with the skip protocol the performance is similar to the baseline NaBOB–TEP without additives. Instead, 2 wt% BS is the one with the highest capacity retention, 49.5% after 200 cycles. On the other hand, the performance of the electrolytes with VEC and TMB is worse than the baseline. As a reference, $NaPF_6$–EC:DEC was also tested, and while with the normal formation protocol its performance was clearly superior to the NaBOB–TEP systems with a capacity retention of 77.4% after 200 cycles, with the skip protocol the retention dropped to 36.7%, a value very similar to the 0.35 M NaBOB–TEP (35.8%). This suggests that the formation protocol has a far-reaching effect on the cycling stability. While the skip protocol is beneficial for the NaBOB–TEP baseline avoiding the unwanted reactions at lower voltage, it affects negatively the performance of the well-known SEI forming additives and solvents, such as EC in the reference electrolyte with $NaPF_6$ or DTD or PES for NaBOB–TEP, which decreases the cycling stability of these electrolytes compared to the normal protocol. On the other hand, the additive BS with the skip protocol is able to improve the performance compared to the

normal protocol and to the baseline electrolyte with the skip protocol. Overall, these results emphasize that the SEI formation mechanism of the electrolyte additives and its passivation behaviour differs depending on the formation protocol.

The cell polarisation evolution of the cells is shown in Fig. 4c and d. The small polarisation values are linked to the good cycling performance, *e.g.* with the 1 M $NaPF_6$–EC:DEC reference that has the best cycling results with the normal formation, the polarisation values stay low and increase only a few mV upon cycling. With the skip protocol, the results show that from the beginning of cycling, the BS sample has low polarisation along with VEC sample, and it remains lower compared to VEC by the 50th cycle, indicating the lower resistance of the cells with BS additive and therefore higher capacity retention.

The rate capabilities of the NaBOB–TEP electrolyte systems in Prussian white–hard carbon pouch cells formatted with the skip protocol were investigated to get an insight to their performance at higher currents. The results in Fig. 5 show that the baseline 0.35 M NaBOB–TEP and the 2 wt% of DTD and PES containing electrolytes enable stable performance up to 1.0C with the specific discharge capacity of the cells being approximately 110 mAh g^{-1}. The BS-containing electrolyte performs quite similarly to DTD and PES samples but due to the better initial capacity, the low C-rate capacities are slightly higher. VEC and especially TMB show lowered rate capability from the beginning of the cycling at lower currents, strengthening the conclusion from the long-term cycling that they might not be the best additives for the NaBOB–TEP system in combination with the skip protocol. 1 M $NaPF_6$–EC:DEC, which is used as a reference, performs relatively similarly to the PES system until 1.0C. At high C-rates above 2.0C, the capacity of the NaBOB–TEP systems drops quickly, reaching ~0 mAh g^{-1} at 4.0 and 5.0C, suggesting that 1.0C is the highest current in which these electrolyte systems can work. The poor coulombic efficiencies (Fig. S12) at higher C-rates also support that. Meanwhile the 1 M $NaPF_6$–EC:DEC is observed to perform well also at higher C-rates (at least until 2.0C, above that the capacity drops rapidly), showing that the rate capability of the PW or HC electrodes is not the limiting factor here. Most of the capacity can be recovered when the cell is cycled afterwards again with 0.2C, which indicates that the capacity drop caused by the high C-rates is not irreversible but more likely caused by the limited kinetics in the system.

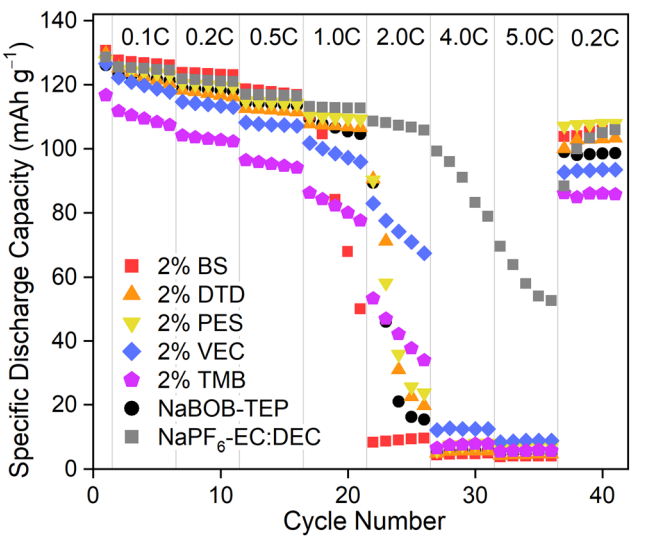

Fig. 5 Rate capability of the NaBOB–TEP electrolyte systems with additives in PW–HC pouch cells with the skip protocol in the first formation cycle.

There are at least three possible causes for the poor capability at higher rates. First, the lower ionic conductivity of 0.35 M NaBOB–TEP compared to the 1 M $NaPF_6$–EC:DEC limiting the performance at higher currents. However, considering that the capacity very quickly drops to zero, there might be other reasons. As previously mentioned, NaBOB is poorly soluble to most common organic solvents. Colbin *et al.*[5] reported that the solubility limit of NaBOB to TEP is somewhere close to 0.38 M, meaning that our selected 0.35 M is relatively close to that limit. A second possibility could be that at high currents, the local NaBOB concentration might exceed the solubility limit, precipitating it and thus hindering the electrochemical processes in the cell but dissolving again at lower C-rates, allowing cycling afterwards. Alternatively, the mobility of Na^+ might be hindered by the TEP solvation, decreasing the charge transfer on the electrode and thus capacity. For now, we do not have a confirmation on the exact reason why the performance at high currents is poor, instead we focus on the SEI formation.

The low-rate capability of the electrolytes does however confirm that during the skip protocol, very little electron transfer will occur during the CC 7.0C charge to 3.0 V (as is also seen in Fig. 3c). This means that most of the electrochemical surface passivation happens afterwards, either during the CV part of the skip protocol when the current drops from 7.0C to 0.1C, or afterwards during the CC at 0.1C. It is likely that some of the compounds forming the SEI during the normal formation protocol with NaBOB–TEP will also be reduced at 3.0 V and form an SEI. However, as the potential of the hard carbon electrode is lower in this case (Fig. S13), the compounds will reduce in different ways and ratios, affecting the SEI formation and composition.

The cyclic voltammograms of the electrolytes, measured using hard carbon as working electrodes to investigate the reduction behaviour of the different systems, are presented in Fig. 6. As expected, the cyclic voltammogram of the baseline 0.35 M NaBOB–TEP (Fig. 6a) shows a strong irreversible reduction peak at 1.25 V *vs.* Na^+/Na during the first scan. This is attributed to the NaBOB reduction as previously mentioned and supported by the literature,[5] and it is not observed during second and third scans, indicating the electrode passivation after the first scan. This peak also has a shoulder at ~1.1 V *vs.* Na^+/Na which based on the study by Ekeren *et al.*[12] is attributed to TEP decomposition. However,

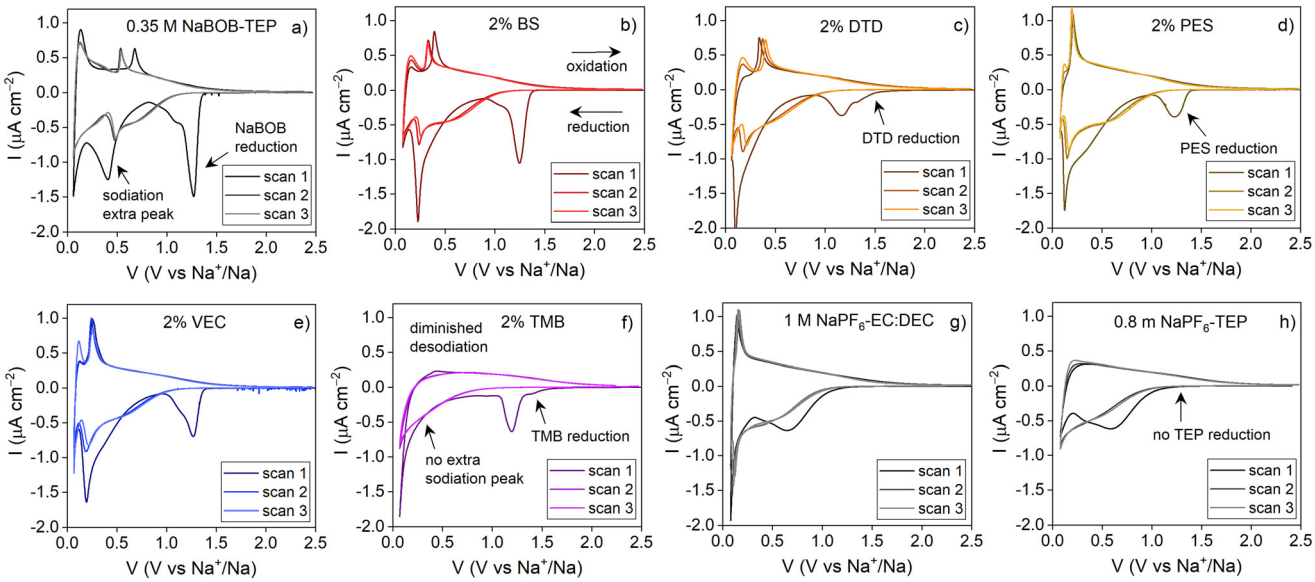

Fig. 6 Cyclic voltammograms of the 0.35 M NaBOB–TEP electrolytes containing a) baseline, b) 2 wt% BS, c) 2 wt% DTD, d), 2 wt% PES, e) 2 wt% VEC and f) 2 wt% TMB. g) 1 M $NaPF_6$ in EC:DEC and h) 0.8 m $NaPF_6$ in TEP. The measurements were performed at scan rate of 0.05 mV s^{-1} in a three-electrode cell using HC as working electrode, PW as counter electrode and partly desodiated PW as the reference electrode.

another reference system with $NaPF_6$–TEP was prepared to further investigate this. The results in Fig. 6h do not show any peak at this potential, suggesting that it is not solely TEP reduction but could be related to the different coordination environment of TEP with different anions.

Furthermore, another reduction peak is observed at 0.4 V *vs.* Na^+/Na with a corresponding oxidation peak in the reverse scan. The reduction current of this peak during the second and third scans is considerably lower, which indicates that the reaction is partly irreversible and passivating. This peak is unexpected, because it does not correspond to the typical hard carbon passivation or sodiation behaviour[18,19] and it is not reported in the previous studies with NaBOB–TEP based electrolytes. It is present in all the NaBOB–TEP electrolytes studied here except for the TMB additive (Fig. 6a–e). To clarify this, we investigated the sodiation and the electrolyte reduction of the same hard carbon electrodes using $NaPF_6$-based electrolytes (Fig. 6g and h) in EC:DEC and TEP. In both of these systems, the current response is similar to the typical HC behaviour, and the additional peak at 0.4 V *vs.* Na^+/Na is not observed. This indicates that the NaBOB salt interaction with the TEP plays an essential role in this process. One possible explanation for this reduction peak is TEP co-intercalation. The peak potential and behaviour match well with the TEP co-intercalation into graphite in Li systems reported by Liu *et al.*,[4] and therefore could indicate something similar happening here with some TEP being co-intercalated into the hard carbon with Na^+. Due to the low solubility of NaBOB and therefore the low concentration in the electrolyte, the solvation shell of Na^+ is expected to be different compared to the high concentration $NaPF_6$–TEP, and could result in more co-intercalation. This should be verified with *e.g.* high-resolution NMR or Raman spectroscopy measurements, however, which are beyond the scope of this paper. Alternatingly, the 0.4 V *vs.* Na^+/Na peak could be caused by the further reduction of the NaBOB–TEP electrolyte, or possibly the reduction of the NaBOB decomposition products combined with TEP, forming the passivating SEI (this would indicate the NaBOB reduction at 1.25 V is not properly passivating). Although we cannot pinpoint the exact cause at this stage, we think this is a more likely explanation for this peak due to its irreversible nature during the first cycle. Finally, as Colbin *et al.*[5] (the only paper reporting the CV of the NaBOB–TEP system) did not observe this peak, it is possible that the composition of the hard carbon affects this process. Nevertheless, the capacity loss caused by this process during the first scan is considerable and explains the poor initial capacities of the cells regardless of the formation protocol used. As a positive side, from the second scan onwards, this peak is relatively stable, indicating that the capacity loss observed during the first scan does not continue with cycling. Finally, a reversible reduction peak is observed at 0.05 V *vs.* Na^+/Na, corresponding to the sodiation of the hard carbon.

The additives affect both the surface passivation and the sodiation behaviour of the hard carbon electrodes. First and foremost, the DTD and PES systems diminish NaBOB decomposition, which is in agreement with the results presented in Fig. 3. In DTD's voltammogram (Fig. 6c), a reduction peak starts at slightly higher potential than NaBOB reduction, at around 1.5 V *vs.* Na^+/Na. This is attributed to the DTD reduction, and the lower current of the NaBOB decomposition peak (compared to the baseline electrolyte) suggests that the DTD decomposition is able to passivate the electrode enough to decrease the NaBOB decomposition. With the PES electrolyte (Fig. 6d), the first reduction reaction

occurs exactly at the same potential as NaBOB–TEP baseline. It is therefore difficult to determine whether PES or the main electrolyte compounds are reduced. In lithium systems PES has been reported to reduce at similar potentials as DTD,[8,20] which might support the idea of PES reducing at this potential. In this case, the broader and diminished reduction peak (compared to the baseline) indicates that not as much NaBOB is reduced, which supports that PES is being reduced. In BS and VEC's voltammograms, NaBOB decomposition is observed, which indicates that these additives do not reduce at earlier or similar potentials than NaBOB. It is quite likely that they would be reduced at lower potentials but as NaBOB is reduced first and at least partly passivates the surface, no additional reduction peaks are observed in BS and VEC CVs. In the case of BS, it could be that the six-membered ring structure of the additive is more stable than the five-membered ring of PES and DTD, which lowers the reduction potential. The work by Yu *et al.*[21] supports this hypothesis as it shows through DFT calculations that the LUMO energy for BS is higher than for PES, meaning that PES is reduced easier. In VEC's case we think that the lack of a double bond in the five-membered ring and sulphur species might result in more stable combination, resulting in a lower reduction potential as well. This indicates that the sulphur species have a positive impact in the SEI formation and stabilisation of the NaBOB–TEP systems. In case of TMB, a small reduction peak is also observed before the NaBOB reduction but it is not passivating as it does not prevent the NaBOB reduction.

The additives also affect the sodiation behaviour. While for the baseline NaBOB–TEP system a reduction peak was observed at ~0.4 V *vs.* Na^+/Na during the first scan, which then shifts to 0.5 V in the following scans, all additives shift this peak to lower potential. In BS, DTD, PES and VEC systems there seems to be a connection between the NaBOB reduction and this peak – the more depressed the NaBOB decomposition peak, the more the sodiation peak is shifted towards the lower voltage. As in the DTD and PES systems the SEI layer has a different composition due to the different reduction reactions, this behaviour suggests that the sodiation mechanism might be affected by the surface chemistry. Simultaneously, however, additive reduction is not observed for the BS and VEC, and the peak is still shifted, which indicates that even if the surface chemistry plays a role in this process, it is not the only contribution. Another factor that could affect the reduction peak potential is the solvation structure of the ions in the electrolyte. While no changes were observed in the FTIR or ^{31}P NMR studies, the additives are still present in the electrolyte and can affect the reactions occurring. Previously, additives have been shown to lower the LUMO energy levels of an electrolyte, leading to lowered reduction potential,[22] and this most likely occurs in this system as well. Whether a higher or lower potential for the reaction is more beneficial to the system, we cannot say.

The behaviour of TMB containing electrolyte differs from the other electrolyte systems considerably. With this electrolyte, only a low-voltage sodiation peak is observed. It is worth noting that the desodiation peak during the oxidation scan is nearly non-existing, meaning that the reaction has a very poor reversibility. This explains the low coulombic efficiency and discharge capacities of the cells containing TMB.

To investigate whether the SEI formation on the hard carbon electrodes has an effect on the surface morphology and the chemical composition when we are using the skip protocol and the additives, the HC surfaces were investigated with SEM and XPS. As the SEI layer formation occurs mostly during the first cycle and that is when the changes in the electrodes are the largest, the pristine, the soaked and skip protocol formatted (desodiated, after 1 cycle) hard carbon electrodes were investigated.

The SEM images of the pristine electrode (Fig. 7a) show that the HC particles have various shapes and sizes, usually between 1–10 μm. The surface does not visibly change after soaking for 24 h in the different electrolyte systems (Fig. 7b and S14), indicating that any possible chemical changes occurring on the surface do not have a significant effect on the morphology. After the formation cycle with the skip protocol, however, some changes can be observed (Fig. 7c–h) compared to the pristine and soaked samples. While the change is small, the surfaces with the baseline, BS, PES and TMB appear rougher compared to the smooth particles seen in the pristine and soaked electrodes. The biggest changes in the morphology are observed in the formatted DTD sample. Here, the hard carbon particles seem to be covered by a layer that smudges the shape of the particles. This indicates that the surface film created by the DTD additive is thicker compared to the other systems to modify the HC surface morphology. Based on the cycling results, however, this does not have a large effect on the cycling compared to the baseline 0.35 M NaBOB–TEP. The skip formatted VEC sample surface (Fig. 7g) seems to be covered with small 50–200 nm particles, which based on their size and shape are attributed to NaBOB crystals (Fig. S5). The origin of these particles is unclear and could not be verified, but they could at least partially explain the poor cycling performance of the VEC containing electrolytes. The SEM images of the Prussian white electrodes were measured as well (Fig. S15). However, no clear changes were observed and as they were not the focus of this study, they were not investigated further.

To investigate the changes in the SEI compositions depending on the additive in the NaBOB–TEP system, XPS measurements were performed for pristine, soaked and with the skip formatted electrodes. C 1s, B 1s, P 2p and S 2s spectra showed the biggest changes and are collected in Fig. 8. Meanwhile O 1s and Na 1s spectra showing only minor changes can be found in Fig. S16. For soaked samples (Fig. 8a–d), large increases in B 1s and P 2p peaks were observed for samples soaked in TMB electrolyte, and a large increase in S 2s and a small increase in P 2p for DTD samples. As in the soaked samples no current is put through the cell, the results suggest that the TMB and DTD additives react with the main electrolyte or the electrodes,

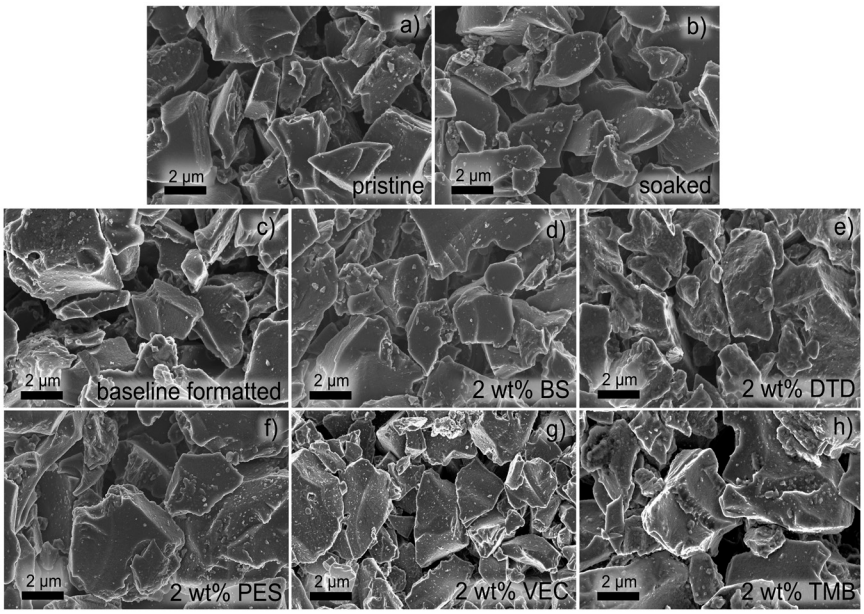

Fig. 7 SEM images of hard carbon electrodes. a) Pristine electrode, b) electrode soaked in the baseline 0.35 M NaBOB–TEP electrolyte. c–h) Electrodes formatted with the skip protocol: c) baseline, d) 2 wt% BS, e) 2 wt% DTD, f) 2 wt% PES, g) 2 wt% VEC, h) 2 wt% TMB.

leading to some of the products precipitating on the HC electrode surface. In TMB's case, the peak attributed to the BO_x environment of boron is observed to increase and shift to lower binding energy compared to the peak from the other electrolytes. This shift could be due to the TMB structure containing boron in a BO_3 environment, compared to the BO_4 environment of NaBOB at 194.6 eV that seems to have precipitated a bit with all soaked samples. However, considering that the amount of additive in the electrolyte is quite small and that an additional peak at lower energy assigned to B–O peak is observed with the soaked TMB sample as well, it is more likely that the TMB, which is a strong Lewis base, reacts with NaBOB in the electrolyte decomposing it. Similarly, TEP does not seem to be stable with TMB either based on the high intensity peaks in the P 2p spectrum. In DTD's case, the P 2p peak is slightly bigger compared to the pristine sample, suggesting DTD reacts with TEP. Furthermore, a lot of sulphur is observed in the S 2s spectrum, indicating DTD decomposes and sulphur species precipitate on the hard carbon electrode. These results are supported by the solution NMR results (Fig. S17) of the electrolytes after 6 weeks of storage time, which show the appearance of new B and P environments and the loss of the original peaks indicating the reaction and decomposition of the electrolyte mixtures with TMB and DTD. The instability of DTD in NaBOB–TEP electrolyte upon storage has also been reported by Welch *et al.*[23] The other three additives, BS, PES and VEC seemed to be stable in the electrolyte system without additional peaks appearing in NMR. Small amounts of sulphur and phosphorus are observed on these soaked electrode surfaces, but those are also observed on the pristine samples, indicating an impurity, most likely from the glovebox where the samples were prepared. Chlorine impurities are observed in nearly all the samples, and caused by impurities in the drying oven during sample preparation.

The XPS spectra of the skip formatted HC electrodes are collected in Fig. 8e–h. The C 1s spectrum for the pristine sample shows a clear peak at 284.5 eV, which is attributed to the sp^2 hybridized graphitic carbon in hard carbon. After formation the peak is diminished and moved to lower binding energy (283 eV), indicating that the SEI is formed and covers the HC electrode, and that sodium is inserted or absorbed to the hard carbon. This sp^2 hybridized peak is barely observed in DTD and PES samples, which indicates that the SEI is either thicker or covering better the hard carbon surface, most likely caused by the reduction of the additives.

In addition to the change in the sp^2 peak, other changes are also observed in the electrodes after the formation cycling. In the pristine electrode, a strong peak is observed at 287.4 eV (C═O/O–C–O), attributed to the surface groups of the hard carbon active material, and in some extent also to the CMC binder used in the electrodes. After formation, regardless of the electrolyte, this peak disappears which further indicates that a passivation layer has been formed with all electrolytes. Simultaneously, the peaks attributed to the carboxyl group at 289 eV and carbonate group at 290 eV increase, which is caused by the decomposition of BOB^- ring structure or subsequent reactions.[24–26] This combined with the increase of Na1s on the HC surface after formation (Fig. S16) indicates the formation of sodium oxalate ($Na_2C_2O_4$) and sodium carbonate (Na_2CO_3) as decomposition products. Meanwhile, the B 1s peak (Fig. 8f) of the formatted electrodes is shifted to lower binding energies compared to the soaked electrodes. This indicates that the boron becomes more

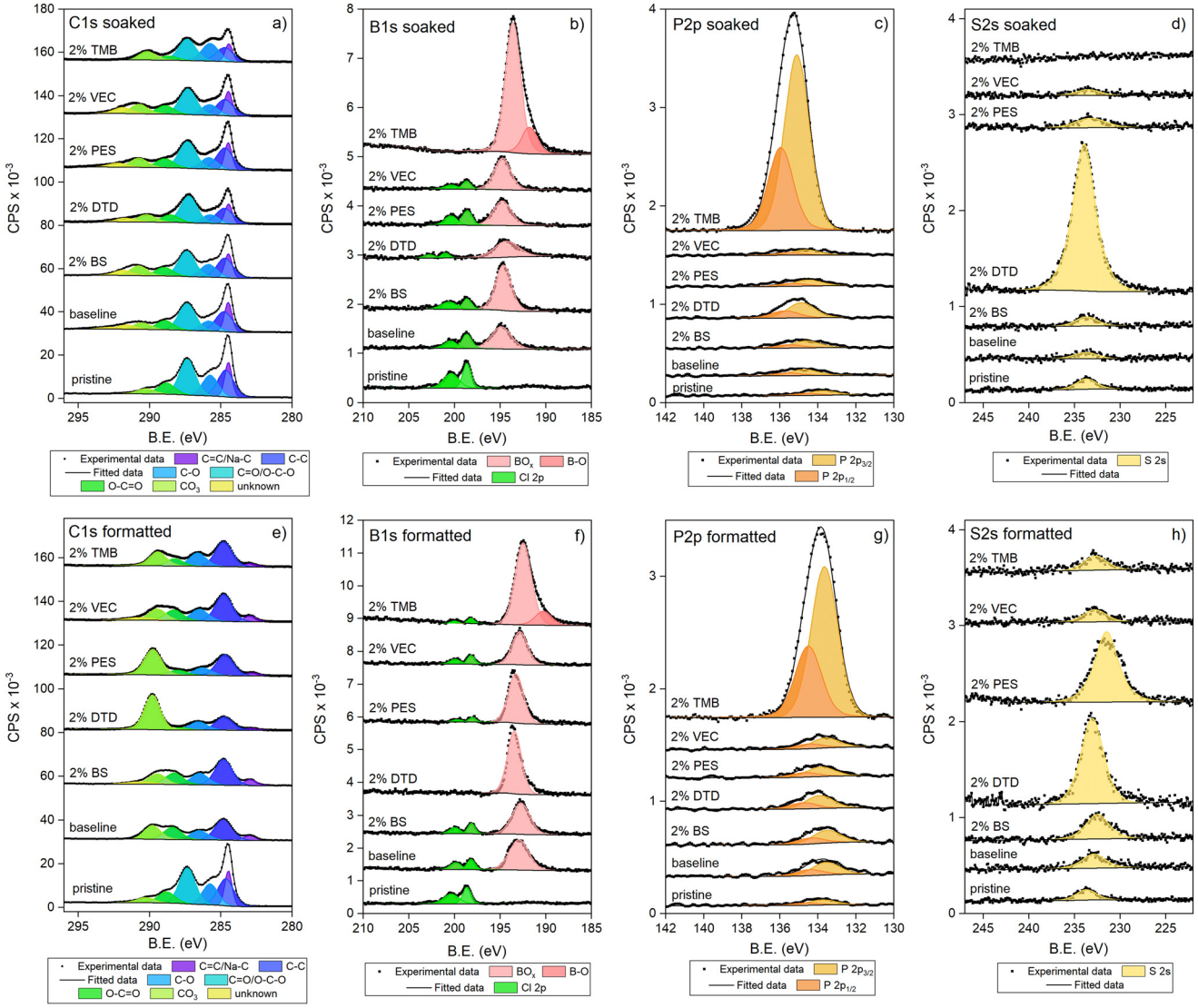

Fig. 8 XPS spectra of the soaked (a–d) & skip protocol formatted (e–h) hard carbon electrodes compared to the pristine electrode. Soaked electrodes: a) C 1s, b) B 1s, c) P 2p and d) S 2s. Formatted electrodes: e) C 1s, f) B 1s, g) P 2p and h) S 2s.

electronegative and that some of the B–O bonds break, which aligns with the breaking of the NaBOB ring structure. Considering that the binding energy of the B 1s remains above 192 eV also after the formation, not all B–O bonds are broken. This suggests the formation of oligomeric boric compounds and boric semicarbonates, similarly to the lithium bis(oxalato)borate (LiBOB) system.[24] In general, our results agree well with the literature on LiBOB, where $Li_2C_2O_4$, and oligomeric borates are reported as the main decomposition products of the salt[24–27] in addition to CO_2 gas.[26]

The additives have a clear effect on the surface chemistry. After the formation, the C 1s carbonate peak is the largest for the PES and DTD samples. At first glance this seems contradictory because in the CV experiments we see that the reduction of NaBOB is prevented by the PES and DTD additives. However, from the study of Colbin *et al.*[5] we know that the carbonate species are mostly formed only after the NaBOB decomposition peak at 1.25 V *vs.* Na^+/Na, indicating that they are formed as a product of reaction(s) that occur later at lower potentials. Melin *et al.*[26] suggest that the carbonate species are formed by a reaction between reduced BOB^- species and other electrolyte components or water impurities. This would mean that as we force the potential of the HC electrode to decrease quickly with the skip protocol, while there are reactive additives present in these electrolyte systems, the rate of these reactions is increased, which could explain the large amount of the carbonate species on the surface of DTD and PES samples. This also leads to a thicker SEI, which is in agreement with the disappearance of the sp^2 hybridized peak in these two samples.

An unknown peak is observed at 292.5 eV and is attributed to an impurity in the NaBOB salt as supported by the C 1s spectrum of NaBOB in Fig. S18. The nature of this species is

uncertain, but we suspect either fluorine or potassium impurity. This peak is present in all soaked samples except with TMB and in the cycled electrodes with the skip protocol with BS and VEC additives, which are the ones with the highest relative intensity of the sp^2 peak. These results suggest that this impurity from the salt remains on the electrodes but it is covered when the SEI is formed. The fact that the peak is present with BS and VEC implies the SEI layer with these additives is thinner than with the others.

The P 2p spectra (Fig. 8g) shows that the amount of phosphorus on the electrode increases slightly after the formation for all electrolytes except for the TMB system which has already a very high intensity in the soaked sample. This suggests that TEP reduction occurs to some degree during the formation cycle regardless of the additive used. The binding energy of 133.6 eV for the P $2p_{3/2}$ is typical for PO_x species which are expected to be formed as decomposition products from TEP reduction and thus agree with the results as well. The decomposition products with TMB–TEP interaction during soaking seem to be further decomposed as well, as the P $2p_{3/2}$ peak is shifted to lower binding energy as well after the formation cycle.

The S 2s spectra (Fig. 8h) show that the SEIs from the DTD and PES samples contain sulphur species. This is a strong indication that the additive reduction takes place also during the skip protocol. However, as shown in Fig. 4b, with the skip protocol these SEI forming additives do not improve the long-term cycling stability. Based on their almost disappearing sp^2 hybridized peaks, the large carbonate peaks and the large S 2s peaks, it is likely that the SEI layer is quite thick, and that together with the large carbonate content nullifies the positive effect of the sulphur-containing species on the interphase, which in turn is reflected in the cycling performance. Meanwhile, the BS sample also contains sulphur, but its amount on the sample surface is considerably smaller. This supports the observations from the CV measurements indicating that BS does not decompose to passivate the HC surface in the same way as DTD and PES, and that BS with a six-membered ring is more stable. Nevertheless, as the sulphur amount on the surface increases, it seems that some BS decomposition does occur during the skip protocol. Based on the CV plot, the NaBOB is reduced first, which could be the reason the overall SEI composition of the BS system looks more similar to the baseline system than the other sulphur-containing additives used in this work. In addition, as the sp^2 hybridized graphitic carbon peak is more visible for the BS system compared to PES and DTD, it is concluded that the BS-sample SEI is thinner which could contribute to the improved cycling data. Finally, it should also be mentioned that sulphur is observed in all the samples, even in those that should be sulphur-free. This is due to an impurity in the glovebox, as sulphur-containing compounds are handled there regularly.

Overall, the cycling performance with the skip protocol in Fig. 4 showed higher capacity retention for the BS additive, while similar performance to the baseline was obtained for the DTD and PES and poorer performance for VEC and TMB. If we consider the changes that the BS additive causes in the skip formatted HC electrodes (electrochemical, morphological and chemical), three apparently small features are found. The first one is the low polarisation in the charge–discharge voltage curves which indicates that the cell resistance is also low. The second one is the small increase of sulphur on the SEI. This change however is small, and assigning it the only cause of a better cycling performance seems unlikely, especially because the DTD and PES contain higher amount of sulfur with slightly poorer cycling stability. The third feature is the reduction potential of the higher potential sodiation peak (0.4 V *vs.* Na^+/Na for the baseline during the first CV scan), which is different for each electrolyte. We observed in the CVs that the stronger passivating additives (DTD and PES) shift this peak towards lower potentials (0.10 V and 0.13 V *vs.* Na^+/Na, respectively) than the weaker ones (BS and VEC at 0.23 V and 0.20 V *vs.* Na^+/Na, respectively). Now, during the skip protocol the cell voltage is forced to 3.0 V, which means that the HC electrode potential drops to around 0.2 V *vs.* Na^+/Na. This means that the skip protocol not only affects the NaBOB decomposition but also the first stage of sodiation (the extra sodiation peak observed in the CV). In the case of the baseline electrolyte 0.35 M NaBOB–TEP, the whole first sodiation phase is forced to a lower potential during the skip protocol while with PES and DTD, part of the sodiation process might occur after the skip. In BS's case, most of the sodiation occurs at the potentials affected by the skip, so in this sense it is more similar to the baseline. The initial capacities of the cells show that the skip protocol is a more effective method in improving the NaBOB–TEP baseline performance, which in turn implies that skipping through the first sodiation phase during the first cycle is beneficial as well. As the BS system enables this feature due to its lesser reactivity, it gains the benefits of the skip formation protocol. This combined with the small amount of sulphur in the thin SEI, seems then a likely cause for the improved capacity retention compared to the baseline and to the traditional SEI forming additives such as DTD and PES.

Conclusions

In this work we investigated the effect of electrolyte additives with different formation protocols on the performance of 0.35 M NaBOB–TEP baseline electrolyte in a Prussian white–hard carbon cell. The results show that the performance of 0.35 M NaBOB–TEP electrolyte can be improved with both approaches, changing the formation protocol and with SEI-forming additives, specifically PES and DTD. However, the skip protocol is shown to be more effective in improving the initial coulombic efficiency of the baseline NaBOB–TEP system and mostly erases the positive effect of the additives when the two improvement methods are combined. Only the BS additive is able to improve the capacity retention of 0.35 M NaBOB–TEP when the skip protocol is used. After 200

cycles the best performing systems with both formation methods (PES for the normal and BS for the skip protocols) provide relatively similar capacity retentions (55% and 50%, respectively), meaning that here the effect of the formation protocol disappears.

The reason why PES and DTD do not improve the cyclability of the skip formatted cells is attributed to their reduction potentials, around 1.4 V *vs.* Na^+/Na, which is higher and occurs before the reduction of NaBOB (1.25 V *vs.* Na^+/Na). While during the normal slow-rate formation protocol the additives have time to react, forming a well-passivating SEI, with the high-rate skip protocol, more NaBOB decomposition takes place with these additives even compared to the baseline system, which then nullifies the positive effect of the sulphur-species from DTD and PES. With the less reactive BS, the amount of NaBOB decomposition stays similar to the baseline, but in addition, a small amount of sulphur-species is generated. This combined with the lower cell resistance and the more similar sodiation behaviour of the baseline and the BS sample, result in better cycling stability when the skip protocol is used.

While DTD is observed to improve the 0.35 M NaBOB–TEP cycling with the normal formation protocol, this additive and TMB react and decompose with the NaBOB–TEP electrolyte. In DTD's case this results in uneven cycling capacities and in TMB's case, the cell capacity drops below 100 mAh g^{-1} in just a few cycles, though after that the capacity is stable. This makes the use of DTD and TMB as additives for 0.35 M NaBOB–TEP unpractical. VEC that we investigated because of its similar structure to VC does not have any positive effect on the performance. Instead it is even slightly negative with the skip protocol compared to the baseline, which could be due to the lack of a stable SEI from this additive.

In addition, the electrolyte additives and also the salt is observed to affect the sodiation behaviour of the hard carbon. When 0.35 M NaBOB–TEP was compared to 1 M $NaPF_6$–EC:DEC, an extra sodiation peak was observed at 0.4 V *vs.* Na^+/Na in the CVs. The additives in the electrolyte shift this peak to lower potentials, larger shift with the better passivating agents such as PES and DTD and smaller with BS and VEC. This indicates that the composition of the SEI formed on the hard carbon affects this process. The reaction is not fully reversible and some of the capacity cannot be recovered during the desodiation, which further explains the poor initial coulombic efficiency of the NaBOB–TEP cells. By understanding the mechanism of this process and increasing its reversibility, the coulombic efficiency of the first cycle and thus the cyclability of the cell could be further improved.

Author contributions

Katja Lahtinen: conceptualisation, investigation, visualisation, writing – original draft, writing – review & editing; Paul Latis: investigation; Lucas Bruylands: investigation; Guiomar Hernández: conceptualisation, funding acquisition, supervision, writing – review & editing.

Conflicts of interest

The authors declare that they have no competing financial interests or personal relationships that could influence the work reported in this paper.

Data availability

The data that supports the findings of this study is available from the corresponding authors upon reasonable request. Supplementary information (SI) is available as well.

Supplementary information is available. See DOI: https://doi.org/10.1039/d5lf00401b.

Acknowledgements

The authors thankfully acknowledge the financial support from the Swedish Energy Agency projects (P2022-00031 and P2024-206030). COMPEL and the Swedish strategic research programme STandUP for Energy are acknowledged for financial support. The authors acknowledge Myfab Uppsala for providing facilities and experimental support. Myfab is funded by the Swedish Research Council (2020-00207) as a national research infrastructure.

References

1 F. Larsson, P. Andersson, P. Blomqvist and B. E. Mellander, *Sci. Rep.*, 2017, **7**, 10018.
2 D. L. Thompson, J. M. Hartley, S. M. Lambert, M. Shiref, G. D. J. Harper, E. Kendrick, P. Anderson, K. S. Ryder, L. Gaines and A. P. Abbott, *Green Chem.*, 2020, **22**, 7585–7603.
3 S. O. L. Colbin, C. A. Hall, A. S. Etman, A. Buckel, L. Nyholm and R. Younesi, *Energy Adv.*, 2024, **3**, 143–148.
4 M. Liu, Z. Zeng, C. Gu, F. Ma, Y. Wu, Q. Wu, X. Yang, X. Chen, S. Cheng and J. Xie, *ACS Energy Lett.*, 2024, **9**, 136–144.
5 L. O. S. Colbin, R. Mogensen, A. Buckel, Y. L. Wang, A. J. Naylor, J. Kullgren and R. Younesi, *Adv. Mater. Interfaces*, 2021, **8**, 2101135.
6 J. Welch, R. Mogensen, W. van Ekeren, H. Eriksson, A. J. Naylor and R. Younesi, *J. Electrochem. Soc.*, 2022, **169**, 120523.
7 A. Buckel, C. A. Hall, L. A. Ma, L. O. S. Colbin, H. Eriksson, R. Mogensen and R. Younesi, *Batteries Supercaps*, 2024, **7**, e202300533.
8 B. Li, M. Xu, B. Li, Y. Liu, L. Yang, W. Li and S. Hu, *Electrochim. Acta*, 2013, **105**, 1–6.
9 A. Freiberg, M. Metzger, D. Haering, S. Bretzke, S. Puravankara, T. Nilges, C. Stinner, C. Marino and H. A. Gasteiger, *J. Electrochem. Soc.*, 2014, **161**, A2255–A2261.
10 P. Y. Zavalij, S. Yang and M. S. Whittingham, *Acta Crystallogr., Sect. B:Struct. Sci.*, 2003, **59**, 753–759.
11 D. Morales, L. G. Chagas, D. Paterno, S. Greenbaum, S. Passerini and S. Suarez, *Electrochim. Acta*, 2021, **377**, 138062.

12 W. W. A. Van Ekeren, L. Dettmann, Y. Tesfamhret, A. J. Naylor and R. Younesi, *Batteries Supercaps*, 2024, e202400489.
13 D. A. Stevens and J. R. Dahn, *J. Electrochem. Soc.*, 2000, **147**, 1271–1273.
14 S. Komaba, W. Murata, T. Ishikawa, N. Yabuuchi, T. Ozeki, T. Nakayama, A. Ogata, K. Gotoh and K. Fujiwara, *Adv. Funct. Mater.*, 2011, **21**, 3859–3867.
15 L. Wang, J. Song, R. Qiao, L. A. Wray, M. A. Hossain, Y. De Chuang, W. Yang, Y. Lu, D. Evans, J. J. Lee, S. Vail, X. Zhao, M. Nishijima, S. Kakimoto and J. B. Goodenough, *J. Am. Chem. Soc.*, 2015, **137**, 2548–2554.
16 Q. Zhang, Z. Wang, X. Li, H. Guo, W. Peng, J. Wang and G. Yan, *J. Power Sources*, 2022, **541**, 231726.
17 P. Janssen, R. Schmitz, R. Müller, P. Isken, A. Lex-Balducci, C. Schreiner, M. Winter, I. Cekić-Laković and R. Schmitz, *Electrochim. Acta*, 2014, **125**, 101–106.
18 S. Alvin, H. S. Cahyadi, J. Hwang, W. Chang, S. K. Kwak and J. Kim, *Adv. Energy Mater.*, 2020, **10**, 2000283.
19 J. S. Weaving, A. Lim, J. Millichamp, T. P. Neville, D. Ledwoch, E. Kendrick, P. F. McMillan, P. R. Shearing, C. A. Howard and D. J. L. Brett, *ACS Appl. Energy Mater.*, 2020, **3**, 7474–7484.
20 A. Sano and S. Maruyama, *J. Power Sources*, 2009, **192**, 714–718.
21 X. Yu, Y. Wang, H. Cai, C. Shang, Y. Liu and Q. Wang, *Ionics*, 2019, **25**, 1447–1457.
22 H. Lohani, A. Kumar, A. Bano, A. Ghosh, P. Kumari, A. Ahuja, A. Sengupta, D. Kumar, D. T. Major and S. Mitra, *Adv. Energy Mater.*, 2024, **14**, 2401268.
23 J. Welch, W. W. A. van Ekeren, J. Mindemark and R. Younesi, *Commun. Chem.*, 2025, **8**, 1–11.
24 K. Xu, U. Lee, S. Zhang, M. Wood and T. R. Jow, *Electrochem. Solid-State Lett.*, 2003, **6**, A144.
25 B. S. Parimalam and B. L. Lucht, *J. Electrochem. Soc.*, 2018, **165**, A251–A255.
26 T. Melin, R. Lundström and E. J. Berg, *J. Phys. Chem. Lett.*, 2024, **15**, 2537–2541.
27 Y.-C. Weng, R. Andersson, M.-T. Lee, J. Mindemark, A. Lindblad, M. Hahlin and G. Hernández, *J. Electrochem. Soc.*, 2024, **171**, 060527.